Journal of Nuclear Materials 377 (2008) 141–146

Contents lists available at ScienceDirect

Journal of Nuclear Materials

journal homepage: www.elsevier.com/locate/jnucmat

Interaction of ⟨100⟩ and ½⟨111⟩ dislocation loops with point defects in ferritic alloys

D. Terentyev *, L. Malerba

SCK CEN, Nuclear Materials Science Institute, Boeretang 200, B-2400 Mol, Belgium

ARTICLE INFO

PACS:
75.50.Bb
61.82.Bg
61.72.Ji

ABSTRACT

The interaction between dislocation loops of interstitial nature with ½⟨111⟩ and ⟨100⟩ Burgers vectors and point defects in Fe has been studied molecular dynamics. Comparative calculations have been carried out using two interatomic potentials for pure Fe ([G.J. Ackland, M.I. Mendelev, D.J. Srolovitz, S. Han, A.V. Barashev, J. Phys.: Condens. Mater. 16 (2004) 1; S. Dudarev, P. Derlet, J. Phys.: Condens. Mater. 17 (2005) 7097]). The results of this study are range and energy of the interaction as functions of size and mutual position of defects. The applied potentials predict somewhat different strain field structure for ⟨100⟩ loops and therefore different lengths of interaction. However, both potentials suggest that, contrary to common belief, the distance of cluster-defect interaction within the glide prism of a ½⟨111⟩ cluster is significantly longer than that of a ⟨100⟩ cluster of similar size, in spite of the longer Burgers vector in the latter case.

1. Introduction

The presence of dislocation loops in pure Fe and ferritic alloys is an essential feature of radiation damage. Two types of dislocation loops are experimentally known to form in these metals, with different Burgers vectors, namely ½⟨111⟩ and ⟨100⟩ [3–5]. The rate of nucleation and growth of these loops defines the evolution of the microstructure in many respects and depends on their interaction (range and strength) with other radiation-induced defects, such as point defects and their small mobile clusters. It is believed that ½⟨111⟩ and ⟨100⟩ loops are sinks with different bias for point defects and that the magnitude of the bias increases with the length of Burgers vector [6,7]. This hypothesis was used to explain the low swelling in bcc Fe and ferritic steels (including high-Cr steels) [7,8]. However, not much is known about the interaction of different types of dislocation loops with point defects and their small clusters at the atomic scale level. It has been shown that self-interstitial atom (SIA) clusters of size up to a few nanometers cannot be described as perfect dislocation loops using an isotropic continuum approach [9], therefore an atomistic approach is required. The interaction of ½⟨111⟩ loops with point defects in bcc Fe has been studied already [9], but it is useful to revise the currently available results in the light of the recent advances in the development of interatomic empirical potentials (EPs) for Fe. On the other hand, no results on the interaction between ⟨100⟩ dislocation loops and point defects are so far available to our knowledge.

In this work a molecular static study of the interaction of ½⟨111⟩ and ⟨100⟩ dislocation loops with point defects in Fe is presented. Comparative calculations have been carried out using two EPs for pure Fe (Ackland, Mendelev et al. [1], and Dudarev and Derlet [2]). The main goal of this study is to estimate range and energy of the interaction as a function of size and mutual position of defects, which can be used in the parameterization of microstructure evolution models.

2. Method

Static calculations were used to estimate the interaction energy between SIA clusters containing up to 442 interstitials and point defects using the molecular dynamics code Dymoka [10]. Calculations have been carried out using two many-body interatomic EPs: one derived by Ackland, Mendelev et al. [1] (henceforth 'Mendelev's potential') and the other by Dudarev and Derlet [2] (henceforth 'Dudarev's potential'). The relaxation of the atomic configurations of interest has been performed at constant volume. The simulation boxes used in this type of calculations contained from 100 to 800 thousand atoms, thereby guaranteeing independence of the result from the box size. In all these static calculations the system was frozen at a temperature close to 0 K using a quench procedure to relax the atomic system at the equilibrium lattice constant. 3D periodic boundary conditions were employed. The results of test calculations of the cohesive energy, the equilibrium lattice constant at zero temperature and the converged formation energy of point defects are given in Table 1 for the mentioned EPs.

* Corresponding author. Tel.: +32 14 333197; fax: +32 14 321216.
E-mail address: dterenty@sckcen.be (D. Terentyev).

0022-3115/$ - see front matter © 2008 Elsevier B.V. All rights reserved.
doi:10.1016/j.jnucmat.2008.02.062

Table 1
Converged values of bulk properties, estimated in a box of 8192 atoms, using constant volume static relaxation

Potential	a_0 (Å)	Cohesive energy (eV)	Formation energies (eV)			
			Vacancy	⟨100⟩ dumbbell[a]	⟨110⟩ dumbbell	⟨111⟩ dumbbell[a]
Mendelev	2.8553	−4.013	1.71	4.17	3.53	4.01
Dudarev	2.866	−4.316	1.97	4.48	3.64	4.13

[a] Constraint has been applied, otherwise the configuration is unstable.

The interaction energy between a point defect (N_1) and a cluster of N_{def} interstitials was estimated as

$$E_{\text{int}}^{N_{\text{def}}+N_1} = E_{\text{form}}^{N_{\text{def}}+N_1} - \left(E_{\text{form}}^{N_{\text{def}}} + E_{\text{form}}^{N_1}\right) \quad (1)$$

where $E_{\text{form}}^{N_{\text{def}}+N_1}$ is the formation energy of the system containing cluster and point defect in the configuration of interest, while $E_{\text{form}}^{N_{\text{def}}}$ and $E_{\text{form}}^{N_1}$ are the converged formation energies of a cluster and a point defect, separately calculated as

$$E_{\text{form}}^{N_{\text{def}}} = E(N_0 + N_{\text{def}}) - E_{\text{coh}} \times (N_0 + N_{\text{def}}) \quad (2)$$

where $E(N_0 + N_{\text{def}})$ is the relaxed energy of a system of N_0 atomic sites containing N_{def} defects (self-interstitials) forming a cluster and E_{coh} is the cohesive energy of the perfect crystal at the equilibrium lattice constant. (Clearly, in the case of the single vacancy $N_1 = -1$.)

3. Results

Since the long range interaction between defects occurs via interplay between their displacement fields, it is useful to recall its main features in the case of ½⟨111⟩ SIA clusters, already studied elsewhere [9] using another EP, and to extend the study to ⟨100⟩ SIA clusters. SIA clusters have platelet shapes and are composed by a collection of parallel crowdions. It is known that the main distortion of the lattice is produced within the cluster glide prism, i.e. within the prism that contains all crowdions and whose axis is parallel to the Burgers vector direction [9], which is ⟨100⟩ or ⟨111⟩ in the cases studied here. This distortion is extended over a long distance from the cluster habit plane that depends on the size of the cluster and, as will be shown, on its Burgers vector as well. The net distortion near a cluster can be attributed to the distortion from each individual defect, which is a ⟨111⟩ or a ⟨100⟩ crowdion, depending on the cluster type. The properties of each individual defect inside the cluster depend on its position in it [11], i.e. a crowdion located at the centre of the cluster will contribute to the displacement field differently from a crowdion located at the edge or somewhere in between. Local distortion also exists outside the glide prism, close to the habit plane of the cluster, in terms of an expanded region. In what follows, we show and discuss the displacement field of ⟨100⟩ and ½⟨111⟩ SIA clusters as reproduced by the applied EPs. Next we shall focus on the interaction of both types of clusters with point defects.

3.1. Displacement field of ½⟨111⟩ and ⟨100⟩ SIA clusters with different interatomic potential

The displacement field produced by a SIA loop can be characterized by the distribution of the relative interatomic distance (RID) between two adjacent atoms along the Burgers vector direction on the line perpendicular to the cluster habit plane (HP), normalized to the equilibrium distance between atoms in the perfect crystal, as has been done in [9]:

$$RID = \frac{x_K - x_{K-1} - b}{b} \quad (3)$$

where x_K and x_{K-1} are the coordinates of the two adjacent atoms along the direction of the Burgers vector of the loop and b is the modulus of the Burgers vector, coincident with the equilibrium distance between them along the chosen direction.

It is known from work done with other EPs that the distribution of the atomic displacements for a defect at the centre of the loop depends on the cluster size. For small clusters (up to a few tens of defects) the largest distortion occurs at the HP, while for larger clusters the maximum is reached a few planes away from the HP. Such a behaviour was observed for ½⟨111⟩ SIA clusters for example in [11,12]. The same effect is found with the presently used EPs and an illustration of this effect is shown in Fig. 1, where the RID distribution as a function of distance from the HP for crowdions located at the centre, middle, edge and near the edge of a ½⟨111⟩ hexagonal SIA cluster of 331 interstitials is presented, as calculated with Mendelev's potential (equivalent results where obtained with Dudarev's). Other test calculations carried out with both EPs have shown that the threshold size of the SIA cluster for this effect to be seen is between 19 and 37 interstitials.

The RID distributions estimated for ½⟨111⟩ clusters of different sizes (from 7 up to 331 interstitials) were found to be practically the same using both Dudarev's and Mendelev's EPs, for all studied positions of the crowdion along the HP. A difference between EPs was found, however, in the RID distribution of the crowdions situated on the HP at the centre and between centre and edge of ⟨100⟩ clusters. The RID distributions are plotted in Fig. 2 for crowdions located in different positions in a ⟨100⟩ SIA cluster consisting of 442 defects, calculated using both EPs. It can be seen that with Dudarev's EP the maximum of the RID for a central defect is located a few planes away from the HP (see Fig. 2(b)), similarly to the case of ½⟨111⟩ loops, while according to Mendelev's EP the maximum value is reached at the centre (see Fig. 2(a)). The absolute value of the RID at the HP was therefore found different from one potential to the other for the defects at the centre of the HP; however, exactly the same result was obtained for the defects at the edge

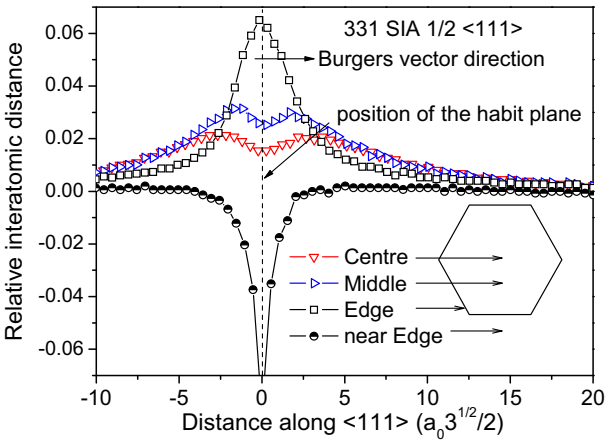

Fig. 1. The RID distribution as a function of distance from the HP for the crowdions at the centre, middle, edge and near the edge of a ½⟨111⟩ hexagonal SIA cluster consisting of 331 interstitials.